Structural and Superconducting Transitions in Mg$_{1-x}$Al$_x$B$_2$

Sergey V. Barabash and David Stroud

Department of Physics, The Ohio State University, Columbus, Ohio 43210

(February 1, 2008)

From systematic *ab initio* calculations for the alloy system Mg$_{1-x}$Al$_x$B$_2$, we find a strong tendency for the formation of a superstructure characterized by Al-rich layers. We also present a simple model, based on calculated energies and an estimate of the configurational entropy, which suggests that the alloy has two separate concentration regimes of phase separation, with critical points near x = 0.25 and x = 0.75. These results, together with calculations of electronic densities of states in several ionic arrangements, give a qualitative explanation for the observed structural instabilities, as well as the x-dependence of the superconducting T_c for $x < 0.6$.

PACS numbers:

The superconducting properties of MgB$_2$ [1] remain the subject of intense research. Although superconductivity in MgB$_2$ (T_c = 39 K) appears to result from a phonon-mediated BCS-like interaction [2–4] the details of this mechanism, including the possible relevance of anharmonic effects [4,5], multiple gaps [5,6] and Fermi nesting [7], are still being investigated. Studying the effects of doping is very important, as it may not only give additional evidence on the origins of superconductivity in pure MgB$_2$, but is also needed to explain the observed structural instabilities [8–10] and experimental difficulties in verifying the predicted increase in T_c with Na or Ca substitutions [4,11].

Alloys of the form Mg$_{1-x}$Al$_x$B$_2$ are the most widely studied experimentally of all the doped MgB$_2$ materials [8–10]. These systems exhibit a variety of unusual behavior. For example, X-ray diffraction results suggest that Mg$_{1-x}$Al$_x$B$_2$ is unstable against phase separation in the concentration range $0.09 < x < 0.25$ and again near $x = 0.7$ [8–10]. Secondly, the superconducting transition shows unusual behavior as a function of x: the transition is broad around $x = 0.25$, consistent with phase separation, then the transition temperature T_c drops sharply *within* the single phase region ($0.25 < x < 0.4$) [9], but superconductivity persists (with $T_c \sim 10$ K) up to $x \sim 0.7$. Thirdly, a superstructure appears to form near $x = 0.5$ [9,10], corresponding to Al ordering in the c direction, and possibly also at other Al concentrations.

In this study we investigate the energetics of Al-doped MgB$_2$, and their possible relation to superconductivity. Our particular aim is, first, to determine which structures have the lowest energy at several concentrations, especially $x = 0.5$ and $x = 0.333$, and, secondly, to use this knowledge to shed light on the phase separation which may occur at small and at large x, and the relation of these structural phase transitions to the loss of superconductivity with doping. While the influence of Al doping on superconductivity in Mg$_{1-x}$Al$_x$B$_2$ has been discussed theoretically by several authors [11–13],

none have considered the effects of these superstructural transitions.

We have carried out *ab initio* calculations of the total energy for several compositions of Mg$_{1-x}$Al$_x$B$_2$, using the Vienna Ab Initio Simulation Package (VASP) [14,15], which employs a plane wave implementation of density functional theory [16]. We used ultra-soft pseudopotentials [17] within the generalized gradient approximation [18]. For all compositions, we first arranged the ions into an ideal MgB$_2$ -like structure, then relaxed the positions of individual ions within a computational supercell until the energy had converged to a chosen tolerance. At most x considered, we did calculations for several possible ionic arrangements, in an effort to determine the energetically favored superstructure.

Our main numerical results are summarized in Table I. For $x = 0$ and 1, our calculated lattice parameters, band structure and density of states are in very good agreement with experiment or with those calculated by other authors. We now discuss our results at other x, starting with $x = 1/3$. In Fig. 1(a), we show the supercell used to model this composition assuming equal concentrations of Al ions in the different Mg layers (entry d in Table I). After ionic relaxation, the B ions shift from their original positions towards the neighboring Al atoms, as indicated by arrows. This behavior is not surprising, since the fully ionized Al^{+3} ions carry an additional $+e$ charge compared to the Mg^{+2} ions, thus attracting the B$^-$ ions. But this ionic relaxation, since it requires altering the length of the strong in-plane σ-bonds formed by the B sp^2 orbitals, is very small (~ 0.01 Å) *in-plane*, with a correspondingly small energy change (~ 0.02 eV per Al).

By contrast, if the Al atoms are assumed to completely fill every third Al/Mg layer [see Fig. 1(b)], the entire B layers shift towards the Al layers by more than 0.1 Å. Table I shows that this relaxation reduces the energy by about 0.2 eV per Al atom. Hence, this layered superstructure is much more favorable energetically than that with Al ions uniformly distributed in the Mg layers.

Similar behavior is observed at other values of x [see Table I and Fig. 1(c)]. The energies of "fully layered" superstructures are always lower than those of structures in which Al is uniformly distributed in the Mg layers, because of this relaxation effect. The large effect of layering is made clear in Fig. 2, where we plot $\Delta E(x) = E_{ground}(x) - E_{lin}(x)$. $E_{ground}(x)$ is the energy per $Mg_{1-x}Al_xB_2$ formula unit of the fully layered ground state superstructure at concentration x, and $E_{lin}(x) = (1-x)E_{MgB_2} + xE_{MgAl_2}$ is the linear interpolation. Clearly, $\Delta E(x)$ is just proportional to the number of B layers situated *between* neighboring Mg and Al layers. This behavior is reasonable, since only these B layers can undergo the preferential relaxation which favors the layered superstructure [19].

Although the fully layered superstructure is always the lowest in energy at any x, one can attain nearly the same reduction in energy by segregating the Al into various partially layered superstructures. We illustrate this point by considering $x = 1/3$. In the fully layered superstructure, the Al ions occupy all the Mg sites in every third Mg layer [Fig. 1(b)]. In an arrangement we denote the "2/3" structure, the Al's fill 2/3 of the sites in every second layer [cf. Fig. 1(d) and Table I]. These two structures have nearly the same energy [20], which is significantly lower than that in which the Al's are randomly distributed in the Mg layers. We now use this fact as the basis of a simple model for phase separation in these alloys, considering for simplicity only the regime $x \leq 1/2$.

At a given value of x, the quantity of interest is the Helmholtz free energy per three-atom primitive cell of the MgB_2 structure, which we write $F(x, T) = E(x) - TS(x)$. We consider a sample that has a total of N_z layers, each

layer having N_ℓ of Mg/Al sites. We assume that $x_z N_z$ of these layers are Al-rich, each with Al concentration x_a, and $(1 - x_z)N_z$ layers are Al-poor, with concentration x_m. In the regime $x < 0.5$, we assume for simplicity that $x_m \sim 0$, from which it follows that $x_a x_z = x$. (When we include x_m as a variable, in a suitably generalized free energy, we find that $F(x, T)$ is minimized by $x_m \sim 0$ for
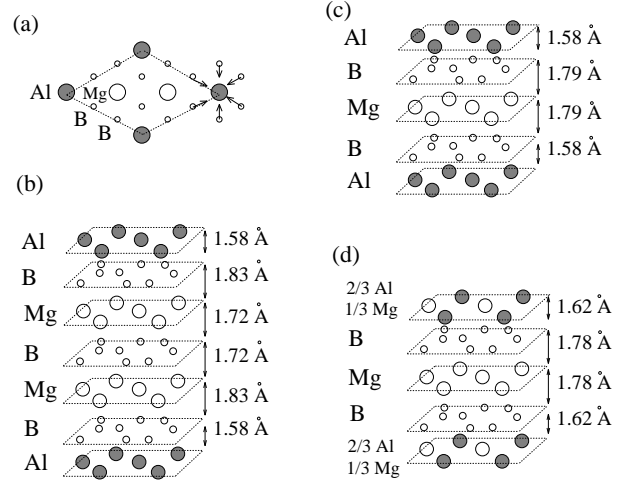

FIG. 1. Some of the $Mg_{1-x}Al_xB_2$ superstructures studied: (a), (b), (c) and (d) correspond to entries *d, g, k* and *f* in Table I. Large circles denote Al (shaded) and Mg (open) ions; small open circles denote B ions. (a) Top view of $x = 1/3$ structure with no Al layering, showing both B and Al/Mg layers (actually separated by c/2 in the c direction). The in-plane displacement of the B ions by ~ 0.01 Å towards the Al ions is indicated by arrows. (b) The ground state superstructure at $x = 1/3$: Al ions occupy every *third* Mg/Al layer; two layers of B's are displaced towards Al's by ~ 0.1 Å. (c) The ground state superstructure at $x = 1/2$. (d) Example of an alternative, higher-energy "2/3 structure" $(x = 1/3)$: The Al ions fill 2/3 of the sites in every *second* Mg/Al layer.

x		superstructure	a, Å	r	E, eV	E_{rlx}, eV
0	a	pure MgB_2	3.07	1.145	-15.416	0
$\frac{1}{5}$	b	fully layered	3.05	1.135	-15.8573	-0.048
$\frac{1}{4}$	c	fully layered	3.05	1.13	-15.9661	-0.050
$\frac{1}{3}$	d	no layering (eclipsed)	3.05	1.105	-16.117	-0.006
	e	no layering (staggered)	3.05	1.11	-16.107	-0.001
	f	partially layered	3.05	1.115	-16.148	-0.042
	g	fully layered	3.04	1.125	-16.1512	-0.067
$\frac{2}{5}$	h	fully layered (2+3 layers)	3.04	1.12	-16.294	-0.074
$\frac{1}{2}$	i	no layering (eclipsed)	3.04	1.095	-16.459	-0.007
	j	no layering (staggered)	3.04	1.10	-16.439	-0.0004
	k	fully layered	3.03	1.11	-16.512	-0.079
$\frac{2}{3}$	l	fully layered	3.02	1.105	-16.772	-0.068
1	m	pure AlB_2	3.005	1.09	-17.245	0

TABLE I. Calculated equilibrium lattice parameters a and $r = c/a$, total energy E per $Mg_{1-x}Al_xB_2$ formula unit, and the change in energy per formula unit E_{rlx} due to ionic relaxation for several possible superstructures of $Mg_{1-x}Al_xB_2$ at different values of x. For entries denoted "eclipsed" (as opposed to "staggered") the Al ions are situated directly above one another in successive Al/Mg layers in the c direction.
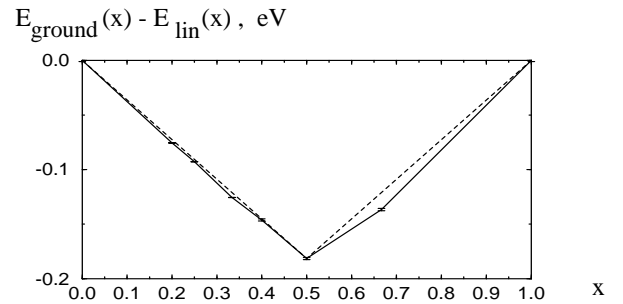

FIG. 2. Energy $E_{ground}(x)$ of the fully layered (ground state) structure per $Mg_{1-x}Al_xB_2$ formula unit, as given in Table I, minus the linear interpolation $E_{lin}(x)$ between the energies of MgB_2 and AlB_2, plotted versus x. The full line simply connects the calculated points, and the dotted line connects the points at $x = 0$, 0.5 and 1.

temperatures up to ~ 500 K [19].)

We assume that the internal energy E does not depend on the arrangement of the Al ions *within* the Al-rich layer, but only on x_z and x_a [21], and we consider only the region $0 \leq x \leq 0.5$. We then make the approximation that

$$E(x_a, x_z) = E_{random}(x) - n(x_z)(E_1 x_a + E_2 x_a^2), \quad (1)$$

where $E_{random}(x)$ is the energy of random $Mg_{1-x}Al_xB_2$. We approximate $E_{random}(x)$ as varying linearly between $x = 0$ and $x = 0.5$, as is approximately true from our numerical results. The second term in eq. (1) is the energy reduction due to superstructural ordering, E_{ord}, discussed above. It is proportional to the fraction of B layers $n(x_z) = 0.5 - |x_z - 0.5|$ which are situated between Al-rich and Al-depleted layers; this effectively bounds the range of possible values of x_z by $x_z \leq 0.5$. From our numerical calculations, E_{ord} is also roughly proportional to x_a. In addition, we allow for a term quadratic in x_a, to insure that the "fully layered structure" has an energy lower than that of "partially layered" structures. This quadratic term is crucial for phase separation. We obtain estimates of E_1 and E_2 from entries d-g from the Table I: we assume that at $x = 1/3$, $E_{random} = \frac{1}{3}E_d + \frac{2}{3}E_e$, $E(x_z = 1/3, x_a = 1) = E_g$, and $E(x_z = 1/2, x_a = 2/3) = E_f$. These relations yield $E_1 \sim 0.1$ eV, $E_2 \sim 0.03$ eV.

We estimate $S(x)$ simply as the sum of the configurational entropies of the individual layers [22]. The standard expression for this entropy of one layer having N_ℓ sites, of which pN_ℓ are occupied by Al ions, is $-k_B N_\ell [p \ln p + (1-p) \ln(1-p)]$. Thus, the total entropy (per $Mg_{1-x}Al_xB_2$ formula unit) is estimated as

$$S = -k_B x_z \left[x_a \ln x_a + (1 - x_a) \ln(1 - x_a) \right] \quad (2)$$

We have numerically minimized the free energy $F(x_a, x_z, T) = E(x_a, x_z) - TS(x_a, x_z)$ for fixed x and T with respect to x_a, subject to $x_a x_z = x$. We call this resulting free energy $F_{min}(x, T)$, and define the quantity $F_{linear}(x, T) \equiv (1 - 2x)F_{min}(0, T) - 2xF_{min}(0.5, T)$, The resulting isotherms of $\Delta F \equiv F_{min}(x, T) - F_{linear}(x, T)$ are plotted in Fig. 3 for several T. They have the classic
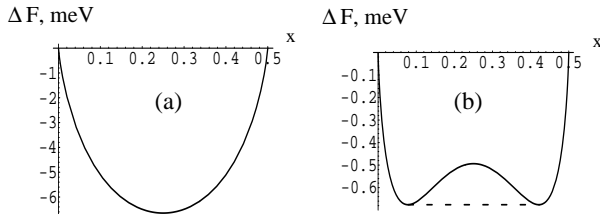

FIG. 3. $\Delta F \equiv F_{min}(x, T) - F_{linear}(x, T)$, as calculated from the model described in the text for (a) $T = E_2 \approx 350$ K; (b) $T = E_2/2.45 \approx 140$ K. The dashed line shows the common tangent construction which determines the composition limits of the two phases in the phase separated region (provided $E_{random}(x)$ is linear in x).

shape associated with phase separation: concave up for $T > T_{inst}$; concave down for $T < T_{inst}$. In the latter regime, the concentrations of the two coexisting phases are determined by the standard common tangent construction sketched in Figure 3. The critical temperature T_{inst} and critical concentration x_{inst} for phase separation are determined as the maximum T, and corresponding x, where $(\partial^2 \Delta F / \partial x^2)_T = 0$. We find $T_{inst} = E_2/2$ (*independent* of E_1), and $x_{inst} = 1/4$. For our choice $E_2 = 0.03$ eV, this procedure gives $T_{inst} \approx 175$ K. The experimental value of T_{inst} is unknown but must exceed the temperature at which a phase separated mixture was reported [8–10] (presumably room temperature). But our estimate is obtained using an extremely simple means of estimating E_2, and would probably be improved by a more elaborate calculation (moreover, our data suggest slight deviation of E_{random} from linear behavior, favoring phase instability).

For concentrations $x > 0.5$, a similar model could also be applied, probably with different parameters E_1 and E_2, leading once again to a region of phase separation with a critical concentration $x_{inst} = 0.75$. On the other hand, the upward curvature in $E(x)$ at $x > 0.5$ (cf. Fig. 2) should oppose phase separation, decreasing the *width* of the two-phase region at a given temperature. This behavior once again appears to agree with experiment, as the observed two-phase region near $x \sim 0.7$ is reported to have much smaller width at comparable T [9].

Finally, we discuss the observed variation of superconducting transition temperature $T_c(x)$ with x, based on these results. Our calculations confirm the suggestion [11–13], that the decrease of T_c with increasing x is due primarily to a reduction in the density of states (DOS) near the Fermi energy. By way of illustration, we show in Fig. 4 our calculated Kohn-Sham DOS $N(\varepsilon)$ in pure MgB_2 and the fully layered $Mg_{0.5}Al_{0.5}B_2$. (We have attempted to minimize structure due to spurious Van Hove singularities produced by the computational algorithm [23,24] by using **k**-meshes as fine as $35 \times 35 \times 35$.) Indeed $N(\varepsilon_F; x = 0.5) < N(\varepsilon_F, x = 0)$ as expected. The observed large *width* $\Delta T(x)$ of the superconducting transition near $x = 1/4$ occurs, we believe, because this concentration lies in the two-phase regime. To some extent, DOS behaves as predicted from the rigid-band model, simply shifting in energy, relative to ε_F, without greatly changing its shape. However, the slightly broader DOS at $x = 0.5$ is, we believe, a real departure from the rigid-band picture, and due to the increased physical unit cell size.

For further insight into the occurrence of superconductivity, we have examined the calculated band structures at different values of x and x_z. We paid special attention to the σ-bonding p_{xy} bands believed to be primarily responsible for the superconductivity. Using a rigid-band model for *small* variations in x at fixed x_z, we found that

for *any* value of x_z, these σ-bands fill at $x \approx 0.6$. (For example, they are filled for structure *l*.) If these were the only occupied bands, the superconducting T_c would seem to vanish above $x \approx 0.6$. Since the electron-phonon coupling constant λ_{p_z} for those bands that remain partially filled at $x > 0.6$ is very small ($\lambda_{p_z} \sim 0.28$ [5]), it could not produce superconductivity for $T > T_{c,p_z} \sim 0.01$ K, according to the Allen-Dynes formula [25,26]. Thus, the persistence of a finite T_c (~ 10 K) may result from some kind of coupling between electrons in the p_z and σ bands. For example, a strong pairing interaction between σ electrons could make it energetically favorable for some electrons to transfer into the p_z band.

To summarize, the present *ab initio* study of $Mg_{1-x}Al_xB_2$ has led to three principal findings. First, we find that at low temperatures a layered superstructure is energetically preferred, not only at $x = 0.5$ as was found experimentally [9,10], but also at other values of x. Secondly, we have described a very simple model for phase separation in these alloy systems. The model is based on a balance between the calculated *ab initio* energies and configurational entropy, and leads to critical points at $x = 0.25$ and $x = 0.75$, also consistent with experiment. Finally, we find that at $x < 0.5$ the experimental trends in both $T_c(x)$ and the width $\Delta T(x)$ of the superconducting transition can be qualitatively interpreted in terms of the calculated x-dependent density of states $N(\varepsilon_F, x)$, but that the interband coupling must be crucial in maintaining finite T_c at $x > 0.6$.
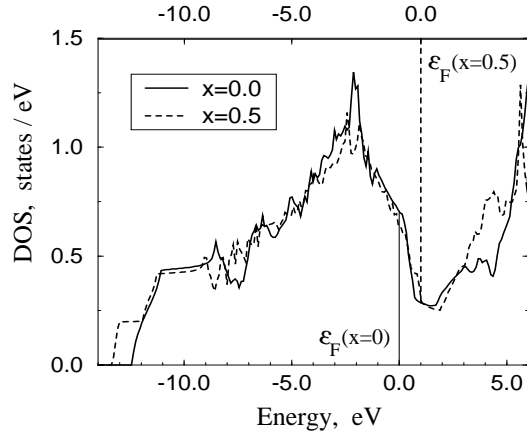
FIG. 4. Electronic density of states $N(\varepsilon, x)$ (per MgB_2 formula unit per spin) for $x = 0$ and for the fully layered superstructure at $x = 0.5$ [the structure shown in Fig. 1(c)]. Vertical full and dashed lines denote ε_F at $x = 0$ and $x = 0.5$. The two curves are lined up so that they each have a filling of eight valence electrons per formula unit at $\varepsilon_F(x=0)$.

[1] J. Nagamatsu *et al*, Nature **410**, 63 (2001).
[2] J.Kortus *et al*, Phys. Rev. Lett. **86**, 4656 (2001); J.M. An and W.E. Pickett, Phys. Rev. Lett. **86**, 4366 (2001).
[3] Y.Kong *et al*, Phys. Rev. **B 64**, 020501 (2001).
[4] T. Yildirim *et al*, cond-mat/0103469 (2001).
[5] A. Y. Liu *et al*, Phys. Rev. Lett. **87**, 087005 (2001).
[6] see, e.g., F. Bouquet *et al*, cond-mat/0104206; F. Giubileo *et al*, cond-mat/0105146; S. Tsuda *et al*, cond-mat/0104489 (2001).
[7] K. Yamaji, cond-mat/0103431; I. Hase and K. Yamaji, cond-mat/0106620 (2001).
[8] J.S. Slusky *et al*, Nature **410**, 343 (2001).
[9] J. Q. Li *et al*, cond-mat/0104320 (2001).
[10] J. Y. Xiang *et al*, cond-mat/0104366 (2001).
[11] J. B. Neaton and A. Perali, cond-mat/0104098 (2001).
[12] S. Suzuki, S. Higai and K. Nakao, cond-mat/0102484 (2001).
[13] G.Satta *et al*, cond-mat/0102358 (2001).
[14] G. Kresse and J. Hafner, Phys. Rev. **B 47**, 558 (1993); G. Kresse and J. Furthmüller, Comput. Mat. Sci. **6**, 15 (1996); G. Kresse and J. Furthmüller, Phys. Rev. **B 54**, 11169 (1996).
[15] We used an energy cutoff of 321eV with **k**-point meshes ranging from $11 \times 11 \times 11$ to $35 \times 35 \times 35$. For a given ionic configuration, these parameters allowed us to attain an energy convergence of less than 1 meV per supercell. For our most accurate calculations, we used a convergence criterion of ~ 0.05 meV per $Mg_{1-x}Al_xB_2$ formula unit.
[16] P. Hohenberg and W. Kohn, Phys. Rev. **136**, 864B (1964); W. Kohn and L.J. Sham, Phys. Rev. **140** 1133A (1965).
[17] D. Vanderbilt, Phys. Rev. **B 41**, 7892 (1990); G. Kresse and J. Hafner, J. Phys: Condens. Matter **6**, 8245 (1994).
[18] J. P. Perdew *et al*, Phys. Rev. **B 46**, 6671 (1992).
[19] S. V. Barabash and D. Stroud (to be published).
[20] In the "2/3 structure", the smaller relaxational gain *per displaced layer* of B's is nearly compensated by the larger number of such layers [cf. Figs. 1(b,d)].
[21] The energy does slightly depend on the particular arrangement of Al's for a fixed x_a (see Table I, entries *d,e* or *i,j*). Our model disregards this weak dependence, and thus aims at describing a typical energy at a given x_a and x_z.
[22] We neglect the entropy associated with the random distribution of the Al-rich layers themselves, since this contribution vanishes in the thermodynamic limit.
[23] R. Haerle and P. Kramer. Phys. Rev. **B 58**, 716 (1998); E. S. Zijlstra and T. Janssen, Europhysics Letters **52**, 578 (2000).
[24] Such spurious structure appears even in pure MgB_2 when the unit cell is simply doubled.
[25] P.B.Allen and R.C.Dynes, Phys.Rev. **B 12**, 905 (1975).
[26] Similar to Ref. [5], we used $\omega_{log} = 56.2$ eV and $\mu^* = 0.13$ for our estimates.